

I give permission for public access to my thesis and for copying to be done at the discretion of the archives' librarian and/or the College library.

---

Signature

---

Date

Relative Levels of Drice Expression During Metamorphosis In Larval Fat Bodies  
of *Drosophila melanogaster*

by

Abigail Bloomgarden

A Paper Presented to the  
Faculty of Mount Holyoke College in  
Partial Fulfillment of the Requirements for  
the Degree of Bachelors of Arts with  
Honor

Department of Biological Sciences

South Hadley, MA 01075

May 2023

This paper was prepared  
under the direction of  
Professor Craig Woodard  
for eight credits.

## Acknowledgements

I would like to thank my advisor Craig Woodard for his guidance, assistance and confidence in me. He encouraged me to continue with my thesis even when it was becoming obvious that my experiments would not yield any data. I have grown professionally and academically during my time in the Woodard Lab, and was able to contribute toward its future by rewriting the western blot protocol for the Woodard Lab. I only hope I have made the lab even half as better as it has made me.

I would like to thank the other members of the Woodard Lab for their support. I would especially like to thank Sarah Luiz and Andie Hardin, who were willing to try out my new and improved western blot handbook.

I would also like to thank the other members of my thesis committee: Professor Amy Camp for providing western blot troubleshooting advice and being moral support and Professor Kerstin Nordstrom, who has supported me since the beginning of my first year, even though I'm not a physics major (sorry).

I would like to thank the members of the Kachimushi Naginata martial arts team for putting up with irregular practice times and a scatterbrained captain.

I would also like to thank Mount Holyoke College and the Department of Biological Sciences for making this research possible.



## TABLE OF CONTENTS

LIST OF FIGURES.....	8
ABSTRACT.....	9
INTRODUCTION.....	10
PROGRAMMED CELL DEATH.....	1
PCD in human diseases.....	1
Necrosis.....	1
Types of PCD.....	2
APOPTOSIS.....	3
Caspases.....	3
IAPs.....	.....
H99 genes.....	.....
“Gas and brake” model.....	.....
DROSOPHILA MELANOGASTER.....	.....
<i>D. melanogaster</i> as a model organism.....	.....
<i>D. melanogaster</i> metamorphosis.....	.....
Ecdysone in PCD.....	.....
Larval fat body remodeling.....	.....
Salivary Gland PCD.....	.....
Non-apoptotic	
WESTERN BLOTTING.....	.....
EXPERIMENTAL DESIGN.....	.....

Previous studies in the Woodard Lab.....	
Method and protein selection.....	
Time point selection.....	
Hypothesis.....	
METHODS AND MATERIALS.....	
SAMPLE COLLECTION.....	
WESTERN BLOTTING.....	
RESULTS.....	
DISCUSSION AND CONCLUSIONS.....	
POSSIBLE RESULTS.....	
HANDBOOK.....	
FUTURE STUDY.....	
LITERATURE CITED.....	

## LIST OF FIGURES

Figure 1. Cytological changes during apoptosis.....	13
Figure 2. The “gas and brake” model.....	15
Figure 3. A western blot using 6 APF salivary glands (right) and fat bodies (left) using anti-Drice, anti- $\alpha$ -tubulin, and 5% dry milk.....	31
Figure 4. A western blot using 0 APF salivary glands (left) and fat bodies (right) using anti-Drice, and 5% dry milk.....	
Figure 5. A western blot using 6 APF salivary glands (right) and fat bodies (left) using anti-Drice, anti- $\alpha$ -tubulin, and 5% BSA.....	
Figure 6. A western blot using 12 APF salivary glands (right) and fat bodies (left) using anti-Drice, anti- $\alpha$ -tubulin, and 5% BSA.....	
Figure 7. A western blot using S2 cell extracts (+ and – actinomycin) and 10 APF salivary glands and fat bodies using anti-Drice, anti- $\alpha$ -tubulin, and 5% BSA.....	
Figure 8. Scenario 1.....	39
Figure 9. Scenario 2a.....	39
Figure 10. Scenario 2b.....	40
Figure 11. Scenario 3.....	40

## ABSTRACT

Programmed cell death (PCD) is the self-destruction of a cell as part of development or maintaining homeostasis. The main drivers of apoptosis are a family of enzymes called caspases. The two main caspases in *Drosophila* are Dronc and Drice. Dronc is an apical caspase, which means it is directly activated by apoptotic signals and in turn activates Drice. Drice is an effector caspase, which means it cleaves certain molecules in the cell which lead to cell death.

During *Drosophila* pupation, larval salivary glands die at 10-12 hours after puparium formation (APF). Unlike most larval tissues, the larval fat bodies of *Drosophila* do not undergo apoptosis. Instead, they remodel, going from a sheet of fat cells to individual cells at around 12 hours APF. Therefore, it would be expected that larval fat bodies would have much lower levels of Drice than larval salivary glands.

In this project, relative levels of Drice protein between *Drosophila* larval salivary glands and larval fat bodies at 0, 6, 10, and 12 hours APF were measured using Western blotting. It was hypothesized that at all time points levels of Drice protein would be lower in the fat bodies than in the salivary glands. Unfortunately, difficulties with the Western blotting protocol and the antibody used led to a lack of statistically significant results. However, troubleshooting of the experiment did lead to revisions of the Woodard Lab Western blotting protocol that will increase the efficacy and efficiency of future blots. Despite the issues with the project, future study in this area would be very valuable and should make use of the updated Western blotting protocol.

## Overview

Programmed cell death (PCD) is the self-destruction of a cell as part of development or maintaining homeostasis (Yalonetskaya et al, 2018). It can be regulated in many ways, from repression of transcription to protein inhibition.

Misregulation of PCD has been linked to many diseases. A lack of necessary PCD is involved in the development of some tumors. As many chemotherapeutic agents work by inducing cell death, this decreased ability to undergo PCD also leads to treatment resistance (Thompson, 1995). When lymphocytes are not removed by PCD, they can become autoreactive and attack other somatic cells (Thompson, 1995). This has been linked to the development of autoimmune diseases such as lupus (Thompson, 1995). On the other hand, too much PCD is linked to degenerative diseases. Many neurological disorders like Alzheimer's, Huntington's, and ALS are characterized by the gradual death of neurons (Thompson, 1995).

In contrast, necrosis is uncontrolled cell death. It can be caused by a variety of external and internal stimuli. The most common causes are mechanical injury to the cell, hypoxia, or chemical agents (Khalid & Azimpouran, 2023). There are two mechanisms of necrosis, both having to do with loss of membrane integrity. The first is an increase in plasma membrane permeability, leading to the collapse of the cationic gradient, which causes the cell to swell and burst (Khalid

& Azimpouran, 2023). The second is disruption of the lysosomes, causing the release of enzymes such as proteases, RNases, and DNases (Khalid & Azimpouran, 2023). This leads to the breakdown of organelles and the eventual death of the cell. This process results in the uncontrolled release of cellular contents into the extracellular space (Khalid & Azimpouran, 2023). Many of these components are pro-inflammatory or otherwise harmful to the surrounding cells. Necrosis is not involved in normal growth and development or in maintaining homeostasis. However, it is associated with several diseases like gangrene, heart attacks, and strokes (Khalid & Azimpouran, 2023).

### **Types of programmed cell death**

Autophagy is a process by which damaged cellular components are engulfed by a double membrane vesicle called an autophagosome (Berry & Baehrecke, 2007). The autophagosome delivers the cellular components to a lysosome where they are degraded and recycled. This process is regulated by *atg* genes (Berry & Baehrecke, 2007). Autophagy is important to cell survival during starvation (Berry & Baehrecke, 2007). However, it is also linked to cell death, the mechanisms of which remain unknown. One theory is that autophagy allows for self-digestion and the removal of cellular debris when phagocytes are not present (Berry & Baehrecke, 2007).

Pyroptosis is characterized by plasma membrane disruption and release of both cellular contents and inflammatory mediators. It typically occurs in phagocytes, keratinocytes, epithelial and endothelial cells (Chen et al., 2022). Like apoptosis, it is driven by caspases that cleave and activate pro-IL-1 $\beta$  and pro-IL-18. Unlike apoptosis, the plasma membrane is disrupted, but the nuclear membrane remains intact. Inflammatory caspases cleave and activate gasdermin proteins (Chen et al., 2022). Gasdermins induce transmembrane pores, disrupting the sodium-potassium balance. The resulting sodium influx also brings water, causing the cell to swell until it bursts. Pyroptosis is associated with inflammation and involved in diseases such as keratitis and glaucoma (Chen et al., 2022).

Necroptosis is characterized by destruction of membrane integrity, and cell and organelle swelling. The morphology is very similar to the uncontrolled necrosis, but necroptosis is in fact a regulated form of cell death. The main triggers of necroptosis are ligands that bind to the death receptor family of proteins. Activated death receptors normally lead to apoptosis, but when caspases cannot be activated, necroptosis is used as an alternate cell death pathway.

Ferroptosis is a form of programmed cell death that is caspase independent. Instead, it is caused by the accumulation of lipid peroxides. Lipid peroxides form when unsaturated membrane lipids come into contact with reactive oxygen species (ROS) generated during normal cellular metabolism

(Hirata et al., 2023). The enzyme that reduces lipid peroxides is called Glutathione Peroxidase 4 (GPX4). When GPX4 is inhibited, lipid peroxides accumulate at the plasma membrane and make it more permeable to cations. The influx of  $\text{Na}^+$  and  $\text{Ca}^{2+}$  and efflux of  $\text{K}^+$  collapses the cation concentration gradient, and the cell ruptures (Hirata et al., 2023). The production of ROS varies depending on the type and environment of the cell. Some tumors produce a large amount of ROS, so inhibitors of GPX4 may have potential as anti-cancer drugs (Hirata et al., 2023).

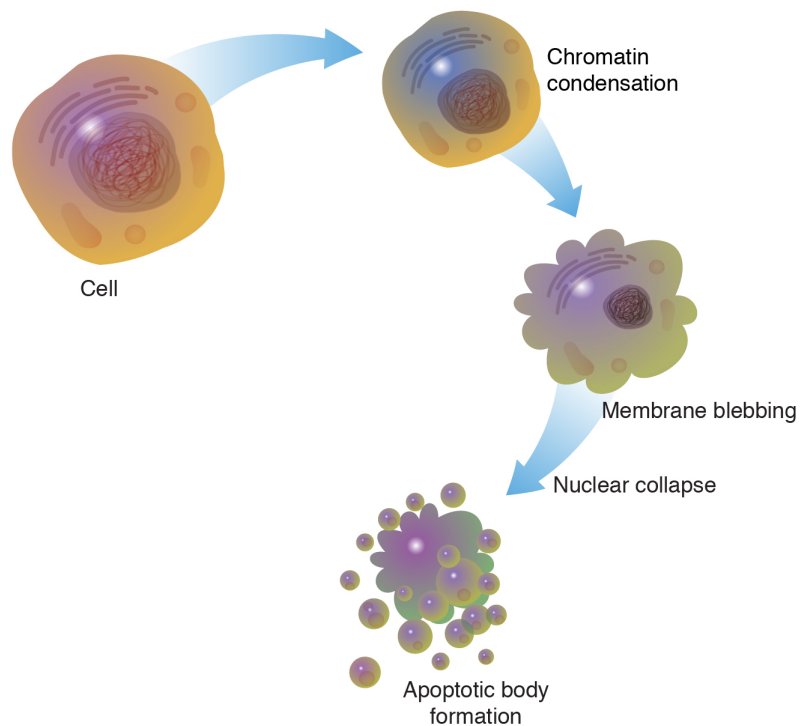


**Figure 1. Cytological changes during apoptosis.** Changes include chromatin

condensation and membrane blebbing. (NHGRI, 2023)

Apoptosis is characterized by cytological features including chromatin condensation, nuclear fragmentation, membrane blebbing, and formation of apoptotic bodies (Yalonetskaya et al., 2018). The main drivers of apoptotic cell death are caspases.

## Caspases

Caspases are a family of cysteine-dependent aspartate-specific proteases. All caspases are synthesized initially as zymogens, the inactive form of an enzyme. These freshly synthesized pro-caspases consist of a variable length prodomain, a p20 subunit, and a p10 subunit (Cashio et al., 2005). Caspases can be sorted into two categories according to their function: apical/initiator caspases and effector caspases. Apical caspases have a long prodomain that contains either a caspase activation and recruitment domain (CARD) or a death effector domain (DED) (Cashio et al., 2005). These motifs allow the apical caspase to be recruited into a larger protein complex. Effector caspases have a shorter prodomain. 7 caspase encoding genes have been discovered in the *D melanogaster* genome:

*dcp-1, dredd, drice, dronc, decay, strica, and damm*. Of these 7, Dronc (*Drosophila* Nedd-2 like caspase) and Dredd (death related CED-3/Nedd2-like) protein are classified as apical caspases (Cashio et al., 2005). Dronc contains a CARD motif in its prodomain, and Dredd contains two DED motifs. However, Dredd appears to be primarily involved in the *Drosophila* immune response. Strica contains a long prodomain, but does not contain either a CARD motif or a DED motif.

Dcp-1, Drice, Decay, and Damm are effector caspases, with a short prodomain. These pro-caspases are activated via cleavage by an apoptosome containing Dronc (Cashio et al., 2005). Effector caspases cleave a specific set of substrates within the cell. This cleavage can either activate or inactivate the molecule. For example, Drice cleaves the inhibitory subunit off of caspase-activated DNase (CAD). Once the subunit is removed, CAD cuts DNA between nucleosomes, leading to apoptosis's characteristic DNA fragmentation (Hengartner, 2000). There are over 100 substrates targeted during apoptosis.

## IAPs

Inhibitor of Apoptosis Proteins (IAPs) are a family of proteins that prevent apoptosis. IAPs share structural motifs. The first of these is the baculoviral IAP repeat (BIR), a sequence of ~80 amino acids. All IAPs possess between one and three of these motifs. Some IAPs also contain Really Interesting New Gene (RING) domains, which have ubiquitin ligase activity. Ubiquitin ligases attach a

protein called ubiquitin to specific substrate proteins. This ubiquitin marks the substrate protein for degradation by a protein complex called a proteasome.

DIAP1, one of the IAPs present in *D. melanogaster*, possesses two BIR domains and a RING domain. The BIR domains are necessary but not sufficient for caspase inhibition. The ubiquitinating activity of the RING domain is also required (Zachariou et al., 2003). The BIR1 domain binds to Dcp-1 and Drice, while the BIR2 domain binds to Dronc (Zachariou et al., 2003). Loss of function mutations in Diap1 cause spontaneous cell death.

## H99 genes

H99 genes are a family of pro-apoptotic proteins in *D. melanogaster*. 3 of the genes in this family actually lie within the H99 locus: *reaper (rpr)*, *head involution defective (hid)*, and *grim*. Another, *sickle (skl)*, is found just outside H99. The fifth, *jafrac2*, is found elsewhere in the genome. The human homolog is *smac*. The H99 proteins aren't homologous to any other proteins. The members of the H99 family vary considerably in length, from Rpr at 65 amino acids to Hid at 439 amino acids long. However, they all share a conserved region at their N-terminals, called the RHG motif. This motif allows H99 proteins to bind to IAPs. Despite this shared motif, each of the H99 proteins appears to have a distinct function. Rpr and Grim block the binding of BIR1 to Drice, but Hid does not.

Jafrac2 also interferes with Diap1-Drice interactions, despite binding to BIR2 (Zachariou et al., 2003). Rpr and Grim bind to BIR1 and BIR2 equally, but Hid, Skl, and Jafrac2 preferentially bind to BIR2 (Zachariou et al., 2003). *hid* mutant embryos have decreased PCD and an increased number of cells in the CNS. On the other hand, *rpr* mutants had a normal amount of PCD and were viable. However, they were sterile due to a behavioral defect caused by an enlarged brain (Zachariou et al., 2003). Thus, none of the H99 proteins alone are sufficient to cause PCD.

### Gas and Brake Model

The separate pieces of the apoptotic puzzle all fit into the “gas and brake” model. The “gas” refers to Dronc’s recruitment into an apoptosome and subsequent cleavage of Drice, which through cleavage of target proteins leads to the death of the cell (Salvesen & Abrams, 2004). This process is normally inhibited by Diap1, the “brake”. An apoptotic signal both “steps on the gas” by activating Dronc and “releases the brakes” by activating the RHG proteins which ubiquitinate and inactivate Diap1 (Salvesen & Abrams, 2004).

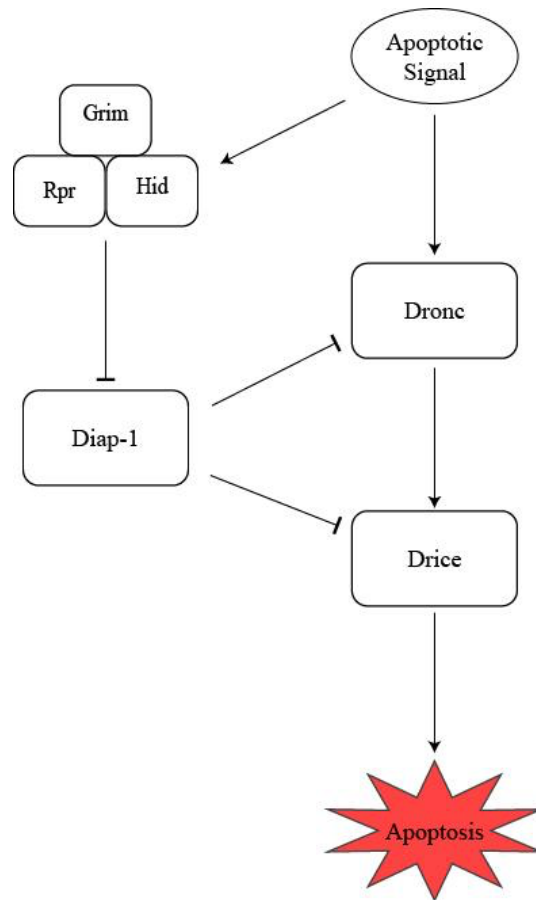


**Figure 2. The “gas and brake” model.** Apoptosis works by simultaneously activating Dronc (gas) and inhibiting DIAP1 (brake).

### *Drosophila melanogaster*

*Drosophila melanogaster* is a common model organism in biology for several reasons. They are easy and cheap to care for, and reproduce rapidly (Jennings, 2011). The entire *D. melanogaster* genome has been sequenced, and was found to be highly homologous to the human genome. As a consequence, many biological mechanisms are conserved between *D. melanogaster* and humans, including the mechanisms that govern PCD (Jennings, 2011). 75% of

human disease genes have functional orthologs in the *D. melanogaster* genome. Mutated strains of *D. melanogaster* are readily available (Jennings, 2011).

### **Metamorphosis**

As holometabolous organisms, *Drosophila* have four distinct life stages: egg, larval, pupal, and adult. Once a larva hatches, it spends the next 5 days eating constantly (Jennings, 2011). The nutrients it consumes are stored in the larval fat body (Aguila et al., 2007). The larva goes through 3 molts during this time. The last of these molts, called the third instar, will eventually leave the food and seek a pupation site (Jennings, 2011). Once it finds a suitable location, the larval salivary glands secrete a glue-like substance that adheres the prepupa (Yalonetsky et al., 2018). The process of pupation lasts for four days (Jennings, 2011), during which the nutrients stored in the fat body are the only source of food (Aguila et al., 2007). The 12 hours immediately after puparium formation (APF) are considered the prepupal stage. The majority of larval tissues, including the salivary glands, would be superfluous in the adult fly. During the prepupal stage, these obsolete tissues undergo PCD (Lee et al., 2002). However, larval fat bodies do not die during this period. Instead, they remodel from single cell sheets to individual cells (Aguila et al., 2007).

### **Ecdysone and PCD**

PCD during *Drosophila* metamorphosis is regulated by the steroid hormone ecdysone. Ecdysone is produced in its inactive form in the prothoracic gland and converted to 20-hydroxyecdysone in the hemolymph by cytochrome P450. Since the active form is most relevant to the topic at hand, 20-hydroxyecdysone will hereafter be called simply ecdysone. Responses to ecdysone are both stage- and tissue-specific. Ecdysone pulses twice during the first 12 hours of metamorphosis (Lee et al, 2002). The first pulse occurs at 0 hours APF (after puparium formation), causing the formation of the puparium and triggering PCD in the larval midgut (Lee et al, 2002). The first pulse of ecdysone at 0 APF activates transcription of the “early genes”: *BR-C*, *E74A*, and *E75* (Lee et al., 2002) These genes then act as transcription factors, causing the transcription of the “late genes”. After the first pulse, ecdysone titers decline, reaching their nadir at 6 APF (Lee et al., 2002). This decrease leads to the transcription of *βFTZ-F1*, which encodes a nuclear hormone receptor. When the second ecdysone pulse occurs at 12 APF, *βFTZ-F1* allows the reinduction of the early genes (Lee et al., 2002). In the salivary gland, these early genes trigger transcription of cell death genes such as *dronc*, *rpr*, and *hid* (Lee et al., 2002). *βFTZ-F1* mutants exhibit a lack of DNA fragmentation in the salivary glands, indicating a lack of Drice activity. However, *BR-C*, *E74A*, and *E75* mutants all showed normal DNA fragmentation (Lee et al., 2002). This may be because these mutants were only deficient in the activity of one of these three proteins. The presence of only two proteins may be enough to activate Drice.

### **Larval fat body remodeling**

Unlike most larval tissues, larval fat bodies do not die during metamorphosis. In *D melanogaster* larvae, fat cells exist in a sheet one cell thick called a fat body. The fat body spans the entire larva, even extending into the head cavity (Nelliot et al., 2006). The individual cells are flat, polygonal, and tightly associated with each other. However, between 0 APF and 4 APF, the fat body begins to retract from the anterior portion of the pupa (Nelliot et al., 2006). Between 4 APF and 6 APF, the fat body retracts from the anterior region completely and the individual fat cells become slightly rounded (Nelliot et al., 2006). Therefore, the span of time from 0 APF to 6 APF is called the retraction phase. At 6 APF, a decrease in ecdysone levels triggers the transcription of  $\beta$ FTZ-F1 (Bond et al., 2011). Between 6 APF and 12 APF, the fat cells become less tightly associated, which is called the disaggregation phase. The pre-pupal to pupal transition occurs at 12 APF due to a second rise in ecdysone levels. The presence of  $\beta$ FTZ-F1 in the fat cells allows this rise in ecdysone to trigger the production of matrix metalloproteinase 2 (MMP2) (Bond et al., 2011). From 12 APF to 14 APF, the fat cells completely detach from each other and become spherical (Nelliot et al., 2006). This is caused by MMP2 degrading the ECM, allowing cell mobility (Bond et al., 2011).

### **Salivary Gland PCD**

Salivary glands are often used for the study of apoptosis in *D. melanogaster*. However, salivary gland cell death is somewhat more complicated than simple apoptosis. Caspases are known to be active during salivary gland death because cells stain with TUNEL, indicating the presence of chromatin condensation (Lee et al., 2002). On the other hand, salivary gland death also involves many autophagic features. Dying salivary gland cells contain many autophagosomes, a hallmark of autophagy (Berry & Baehrecke, 2007). Both *atg* and caspase genes are induced during salivary gland death. When caspases are inhibited, salivary glands are still partially degraded (Berry & Baehrecke, 2007). When *atg* genes are inhibited, salivary glands are still partially degraded (Berry & Baehrecke, 2007).

Although salivary gland PCD is not just apoptosis, previous experiments in the Woodard Lab used salivary glands as their positive control (Han, 2019; Alexander, 2021; Kiran Cavale, 2022). In order to compare the findings of this study with those studies, salivary glands should be used as a positive control. Additionally, there is evidence that Drice is present and active in salivary gland death (Lee et al., 2002). While they may not be an example of pure apoptosis, salivary glands can still serve as an example of Drice activity during metamorphosis, which is the focus of this study.

### **Non-apoptotic functions of Drice**

*D. melanogaster*, along with other arthropods, possess organs called the Malpighian tubules (MTs). MTs are single layered epithelial tubes. Two of the types of cells MTs are composed of are Type I principal cells (PCs) and Type II stellate cells (SCs), which are typically arranged in a pattern (Ojha & Tapadia, 2021). MTs are responsible for excretion and osmoregulation in both larval and adult *D. melanogaster* (Ojha & Tapadia, 2021). Due to this continued function, MTs are one of the few types of larval tissues that does not undergo apoptosis during the prepupal to pupal transition (Ojha & Tapadia, 2021). However, one of the changes that does occur is a remodeling of the SCs, going from “cuboidal” in the larval stage to “star shaped” in the adult (Ojha & Tapadia, 2021).

Sublethal Drice activity has been detected in MTs. Homozygous Drice mutants showed notable differences in their MTs (Ojha & Tapadia, 2021). Tubules were shortened, misshapen, bulging, or even entirely collapsed. SCs in Drice mutants remodeled prematurely, becoming star shaped in third instar larvae instead of during pupation (Ojha & Tapadia, 2021). Drice mutants also had irregular arrangement of PCs and SCs, forming clumps instead of appearing at regular intervals (Ojha & Tapadia, 2021). Third instar mutant MTs had disorganized cytoskeletons. Actin filaments were denser, and distributed irregularly around the SCs (Ojha & Tapadia, 2021).

### **Western blotting**

Western blotting is a technique used to identify and quantify the presence of a protein. First, the tissue of interest (in this case, larval salivary glands and fat bodies) is collected and the cells are lysed to extract the protein. This is done in a protease-inhibiting solution in order to prevent degradation of the proteins (Mahmood & Yang, 2012). The sample is then combined with a loading buffer and heated to denature the proteins. The loading buffer contains sodium dodecyl sulfate (SDS), which acts as a denaturing agent and as a surfactant to give all of the proteins the same negative charge (Mahmood & Yang, 2012).. Glycerol allows the sample to settle into the wells of the gel. Bromophenol blue allows the sample's progress through the gel to be tracked. A reducing agent such as beta-mercaptoethanol, is also added and facilitates denaturing by breaking disulfide bonds (Mahmood & Yang, 2012). The sample is added into the wells of a polyacrylamide gel, which is relatively porous. A protein ladder, made up of dyed proteins of known kDa, is also added. A current is then applied, with the negative electrode at the top of the gel and the positive electrode at the bottom. The negatively charged proteins migrate away from the negative electrode and towards the positive electrode. Proteins with a lower kDa travel more easily through the gel than ones with a higher kDa, so smaller proteins end up lower down in the gel (Mahmood & Yang, 2012).

Once the proteins have been separated by size, the gel is placed against a membrane and a current is applied perpendicular to the gel, with the positive

electrode on the membrane side. The proteins migrate towards the positive electrode, off the gel, and onto the membrane (Mahmood & Yang, 2012).

The membrane is then placed in a blocking buffer, usually 5% skim milk in TBST. The blocking buffer adheres to places on the membrane where there is no protein which prevents non-specific antibody binding and therefore reduces background signal (Mahmood & Yang, 2012).

The membrane is removed from the blocking buffer and placed in the primary antibody solution. The primary antibody solution contains the antibody for the protein of interest, and typically an antibody for a loading control (Mahmood & Yang, 2012). A loading control is a “housekeeping protein” that the different tissues being tested should have in equal amounts. Therefore, if 3x as much loading control is detected for one sample, that means there is 3x as much protein in that sample overall, and the results for the protein of interest can be interpreted in that context. The primary antibodies are suspended in a blocking solution. 5% bovine serum albumin (BSA) in TBST is often used (Mahmood & Yang, 2012). Since BSA is pure protein, it is preferred for a primary antibody solution over skim milk, which contains other substances that could interfere with antibody binding (Mahmood & Yang, 2012).

After the membrane is incubated in the primary antibody solution, it is removed and washed in TBST to remove excess antibody. It is then placed in the secondary antibody solution. The secondary antibody binds to the primary antibodies (Mahmood & Yang, 2012). Usually it is an antibody to whatever

animal the primary antibodies were produced in. For example, the two primary antibodies in this study were rabbit-derived, so the secondary antibody is anti-rabbit. The secondary antibody solution can be 5% skim milk, because lower concentrations are needed. The secondary antibody is conjugated to an enzyme called horseradish peroxidase (HRP) (Mahmood & Yang, 2012).

After the membrane is incubated in the secondary antibody solution, it is washed again in TBST to remove excess antibody. A solution is added to the membrane composed of peroxide and luminol. These chemicals react with HRP to produce a faint light, which can be captured by an imager (Mahmood & Yang, 2012).

### **Previous research and experimental design**

In the Woodard Lab, Ashley Han (2019) and Grace Alexander (2021) both attempted to measure the levels of *diap1* and *dronc* transcription in the fat bodies of *D melanogaster* using qRT-PCR. qRT-PCR measures the amount of transcription of a particular gene. However, for various reasons, neither study could be completed. Shweta Kiran Cavale (2022) also attempted the same study but the *diap1* primers did not work. Furthermore, qRT-PCR cannot measure the amount of gene product present in the cell, nor whether that protein has undergone any posttranslational modifications. As post-translational modification via cleavage is key to the function of caspases, there is a risk that qRT-PCR alone may not give the full picture of what's happening in a particular tissue. Therefore

this study made use of western blotting, which can measure levels of a particular protein and (most) posttranslational modifications.

Although the previous experiments tested for *diap1* and *dronc* mRNA, there are no commercially available antibodies for Diap1 or Dronc protein. However, antibodies that bind to uncleaved and cleaved Drice are available. Since Dronc is the only known enzyme that cleaves Drice, the presence of cleaved Drice in a sample can act as an indirect sign of Dronc activation.

Time points were chosen based on developmental timing. The first ecdysone pulse occurs at 0 h APF, then ecdysone levels decline, reaching their lowest point at 6 h APF. The second ecdysone pulse occurs at 12 h APF. After outside consultation, a fourth time point was selected at 10 h APF. This is around the time that the individual fat cells completely detach and change shape. As Drice may be involved in regulating cell shape changes in other tissues, 10 APF may be a good time to observe the level of Drice activity in the fat body.

This study is intended to complement Han (2019), Alexander (2021), and Kiran Cavale (2022) by examining posttranslational regulation of PCD in the fat bodies of *D melanogaster* during metamorphosis. It is expected that levels of Drice in general and cleaved Drice specifically will be the same in fat bodies and salivary glands for the first 10 hours APF. After the second ecdysone pulse, levels of Drice, cleaved and uncleaved, will rise in salivary glands, while Drice levels in the fat body will remain negligible. However, Drice has many non-apoptotic

functions, including remodeling in another tissue that does not undergo PCD during metamorphosis. Therefore, there is a possibility that there may be a sublethal activation of Drice in the fat body.

## MATERIALS AND METHODS

Canton S *Drosophila melanogaster* stocks were raised on standard fly food and kept at 25°C. Prepupae were either dissected at 0 APF or aged for 6, 10, or 12 hours at 25°C. At each time point, larval fat bodies and salivary glands were collected from 3 pupae in 1x PBS. Samples were placed into microcentrifuge tubes containing 15 µl of a solution composed of 98% 1x RIPA buffer, 1% protease and phosphatase inhibitor, and 1% EDTA. Tubes were labeled with the date, type of tissue, and time APF. Samples were stored at -80°C until used.

To prepare samples for western blotting, 14.6 µl of Laemmli buffer and .4 µl beta-mercaptoethanol were added. Samples were heated at 90°C for 10 minutes, spun to bring down condensation, and placed on ice. 25 µl of each sample and 15 µl of protein ladder (PageRuler™ Prestained Protein Ladder, ThermoFisher Scientific, Cat #26616) were run on a PAGE gel (Any kD™ Mini-PROTEAN® TGX™ Precast Protein Gels, Bio-Rad, Cat #4569033) in a gel electrophoresis rig. Running buffer was composed of 100 ml 10x Tris/Glycine/SDS buffer (Bio-Rad, Cat #1610732) and 900 ml ddH<sub>2</sub>O. Samples were run at 120 V for two hours.

Proteins were transferred to a nitrocellulose membrane (Thermo Scientific™ Nitrocellulose Membranes, 0.2 µm, 8 x 8 cm, Cat #88024) in transfer buffer at 30V for one hour. Transfer buffer was composed of 100 ml 10x

Tris/Glycine buffer (Bio-Rad, Cat. #1610734), 200 ml methanol, and 700 ml ddH<sub>2</sub>O. Membrane was agitated for one hour in 40 ml blocking buffer composed of 40 ml TBST (1x Tris-buffered Saline and 0.1% Tween 20) and 2 g dry milk powder.

The membrane was incubated in 40 ml of primary antibody solution at 4°C overnight. Originally, the primary antibody solution was composed of TBST, 5% skim milk powder, anti-Drice antibody (Cell Signaling Technology, Cat #13085) at 1:2000 concentration, and anti- $\alpha$  tubulin antibody (Abcam, Cat#52866) at 1:5000 concentration. It was later discovered that the concentration of anti-Drice should be double what was previously used. It was also discovered that bovine serum albumin allowed for greater clarity of the signal. Subsequent trials used a primary antibody solution composed of TBST, 5% BSA, anti-Drice antibody at 1:1000 concentration, and anti- $\alpha$  tubulin antibody at 1:5000 concentration. In order to conserve antibodies, 20 ml of solution was used per blot.

The membrane was washed 3x with 25 ml 1x TBST for 10 minutes each time. The membrane was then incubated in the secondary antibody solution for 2.5 hours. Secondary antibody solution was composed of TBST, 5% skim milk powder, and anti-rabbit antibody at 1:7500 concentration. Once removed, the membrane was washed 3x with 25 ml 1x TBST for 10 minutes each time.

The membrane was then washed with 25 ml 1x TBST three times for 10 minutes each.

The ECL reagent (Clarity Max Western ECL Substrate, Bio-Rad, Cat#1705062) was prepared with 1 ml peroxide solution and 1 ml luminol solution and added evenly onto the membrane. The membrane was imaged with an Azure Biosystems 600 imager. For use in this thesis, images were resized using Adobe Photoshop.

## RESULTS

The first western blot was performed with 6 APF salivary glands and fat bodies using the original primary antibody solution. Only one band was visible at 55 kDa in either lane. The location of the bands led to the conclusion that they were showing  $\alpha$ -tubulin. No bands were found at 38 kDa or 21 kDa, indicating that either neither uncleaved or cleaved Drice was present, or the antibody was not functional.

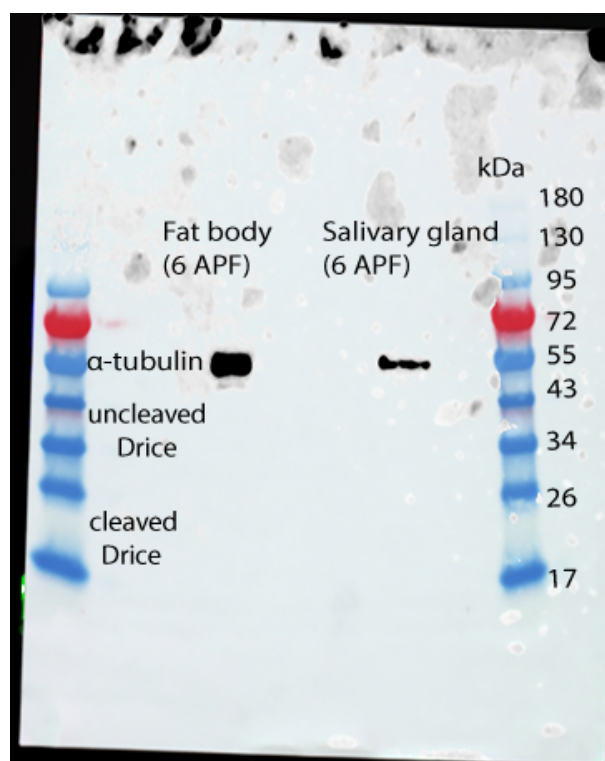


**Figure 3. A western blot using 6 APF fat bodies and salivary glands using anti-Drice, anti- $\alpha$ -tubulin, and 5% dry milk. One band of  $\alpha$ -tubulin is visible in both the fat body and the salivary gland lanes, and no Drice is visible.**

A western blot was subsequently performed with 6 APF salivary glands and fat bodies and using a primary antibody solution similar to the original, but

without the anti- $\alpha$ -tubulin antibodies. This was done in order to test the effectiveness of the anti-Drice antibody. No bands were visible on this blot.

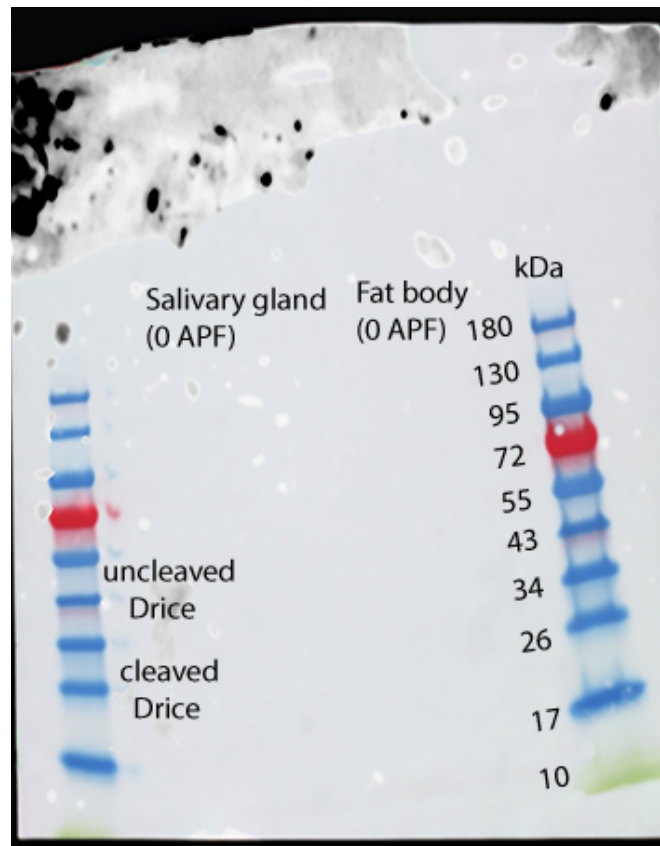


**Figure 4. A western blot using 0 APF salivary glands and fat bodies using anti-Drice and 5% dry milk. No bands are visible on the blot.**

After some investigation, it was discovered that the initial ratio of anti-Drice antibodies was half of what it should have been. Additionally, it was possible that the dry milk in the primary antibody solution was interfering with antibody binding, and BSA would be more optimal. Therefore, the primary

antibody solution was revised to the new ratio of anti-Drice antibodies and the use of 5% BSA.

A western blot was performed with 6 APF salivary glands and fat bodies using the revised primary antibody solution. Two strong bands were visible in the salivary gland lane, and two strong bands and one faint band in the fat body lane. As the strong bands in both lanes were between 55 and 43 kDa, it was determined that they were the two isoforms of  $\alpha$ -tubulin. The identity of the third faint band is unknown, but it has been documented to show up with the anti- $\alpha$ -tubulin antibodies. However, no Drice bands were present.

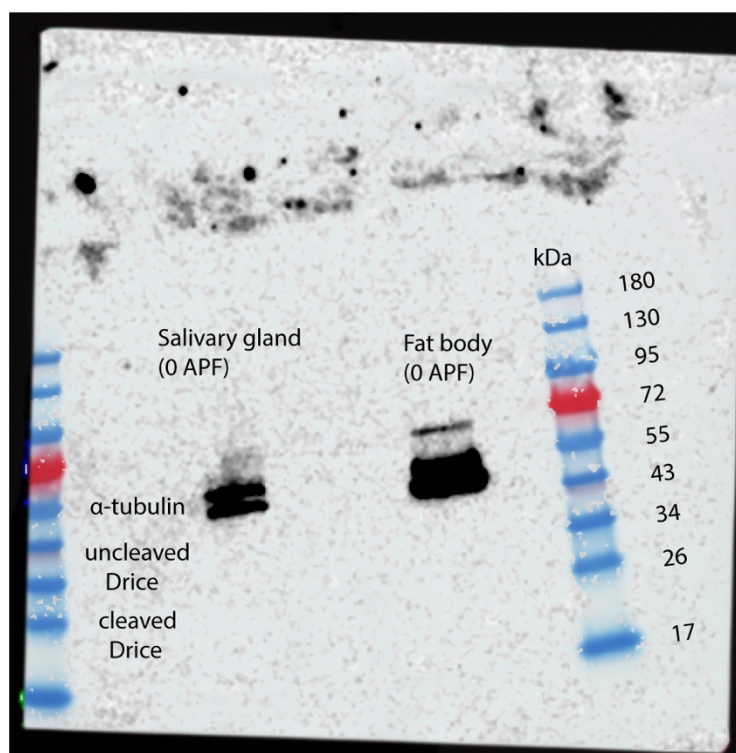


**Figure 5. A western blot using 6 APF salivary glands and fat bodies using anti-Drice, anti- $\alpha$ -tubulin, and 5% BSA. Two bands of  $\alpha$ -tubulin are visible in**

the salivary gland lane, and 3 are visible in the fat body lane. No Drice is visible. Red boxes indicate where the bands of uncleaved Drice should be, and blue boxes indicate where the bands of cleaved Drice should be.

Although some amount of uncleaved Drice exists in all cells (Thompson, 1995), it was possible that the amount of uncleaved or cleaved Drice in 6 APF fat bodies and salivary glands was too low to be picked up by a western blot. To account for this, a western blot was performed with 12 APF fat bodies and salivary glands using the revised primary antibody solution. The  $\alpha$ -tubulin bands were somewhat fainter than the 6 APF, but no Drice bands were found. As 12 APF is the peak of PCD in salivary glands, it would be very unlikely that no Drice would be present.

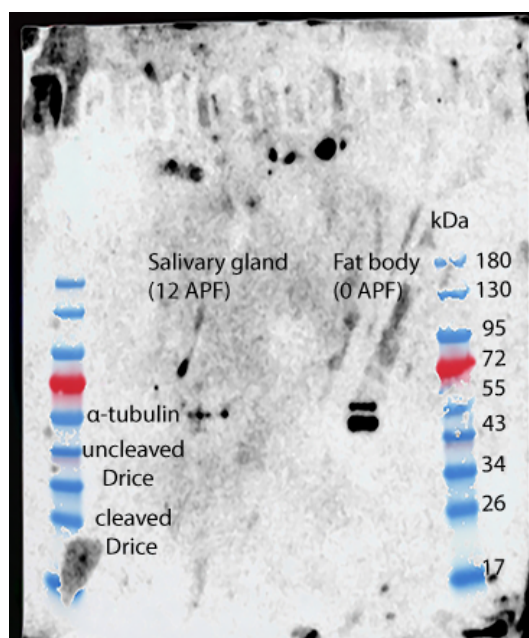


**Figure 6. A western blot using 12 APF salivary glands and fat bodies using anti-Drice, anti- $\alpha$ -tubulin, and 5% BSA. One band of  $\alpha$ -tubulin is visible in the salivary gland lane and two in the fat body lane. No Drice is visible.**

At this time Cell Signaling Technology, the manufacturer of the anti-Drice antibody, was contacted. In order to test the effectiveness of the antibody, they sent two vials of cell extracts, one without actinomycin (uncleaved Drice only) and one with actinomycin (both cleaved and uncleaved Drice). A western blot was run with both extracts and 10 APF fat bodies and salivary glands using the revised primary antibody solution without anti- $\alpha$ -tubulin antibodies. No signal was observed. It was concluded that the anti-Drice antibody was non-functional. Unfortunately, due to the approaching end of the semester, a replacement vial of antibodies was not feasible.

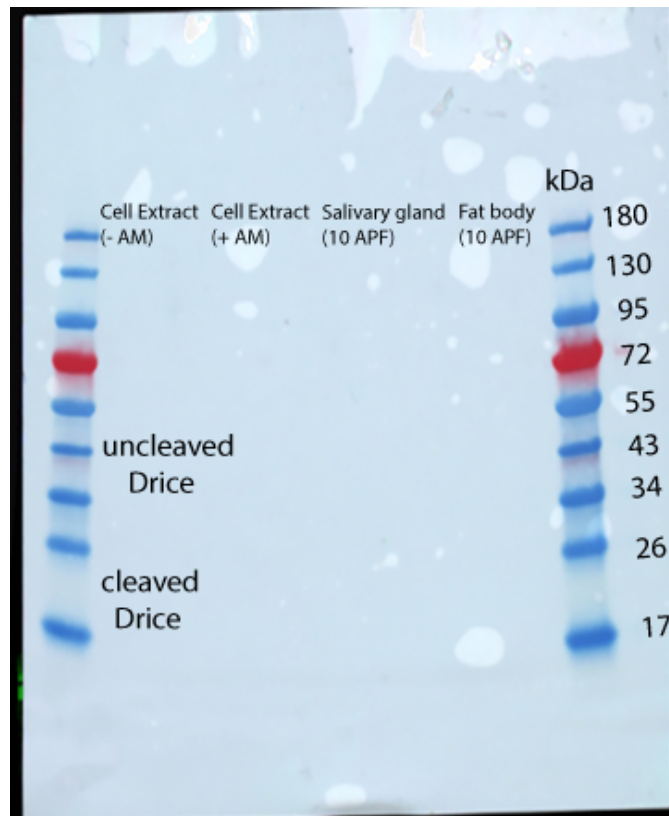


**Figure 7. A western blot using S2 cell extracts (+ and – actinomycin) and 10 APF salivary glands and fat bodies using anti-Drice and 5% BSA. No bands of Drice are visible in any of the lanes.**

## **DISCUSSION AND CONCLUSIONS**

Since there is some level of Drice present in all tissues (Thompson, 1997), it is difficult to speculate about the relative levels of uncleaved Drice in the fat bodies and salivary glands. However, Drice is only cleaved when it is activated, making the presence of cleaved Drice an indicator of Drice activity. In salivary glands, the amount of cleaved Drice should be negligible for the first 10 hours APF, reflecting the lack of PCD at that time. As the process of PCD begins in the

salivary glands, the amount of cleaved Drice should rise sharply, as the H99 proteins inhibit Diap1 and allow Dronc activity. Cleaved Drice levels should remain high until the salivary glands fully degrade.

As for the amount of cleaved Drice in the fat body, there are a few hypothetical scenarios for how it may or may not vary during metamorphosis. The first scenario (Fig. 9, Appendix) is that levels of cleaved Drice in the fat body remain negligible throughout metamorphosis. The fat body progresses through the retraction, disaggregation, and detachment phases without the need for Drice activity. The second scenario is that levels of cleaved Drice in the fat body rise after the first pulse of ecdysone at 0 APF. This could implicate it in the retraction phase from 0 to 6 APF (Fig. 10, Appendix), whether involved in the retraction itself or the slight rounding of the individual fat cells. Or it could be implicated in the disaggregation phase from 6 to 10 APF (Fig. 11, Appendix), loosening the associations between fat cells. The third scenario (Fig. 12, Appendix) is that levels of cleaved Drice in the fat body rise after the second pulse of ecdysone at 10-12 APF. This would implicate it in the detachment phase, either in the complete detachment of the individual fat cells or in the cells becoming fully spherical.

Of these three scenarios, only the first has any evidence behind it. Even then, it is essentially an absence of opposing evidence; larval fat bodies do not undergo PCD, therefore Drice activity is not high enough to be lethal. Without

actual western blot data, it's difficult to know whether Drice activity in fat bodies is elevated above the norm during metamorphosis.

Although this study failed to produce any data, the process of troubleshooting led to improvements to the Woodard Lab's western blot protocol. A new handbook has been developed that will hopefully increase the efficacy and efficiency of western blotting for future students.

Future research into this topic should use the updated western blotting protocol. Additionally, future studies should also examine 14 APF pupae. Although 12 APF is the peak of remodeling in fat bodies and PCD in salivary glands, those processes do continue until around 14 APF (Nelliot et al., 2006; Lee et al., 2002). In order to accurately represent the levels of Drice during metamorphosis in fat bodies and salivary glands, both tissues should be analyzed at 14 APF. However, the diminished amount of salivary glands in 14 APF pupae may necessitate the dissection of more than 3 prepupae. It may also be prudent to test the anti-Drice antibodies using the remaining cell extracts.

## APPENDIX

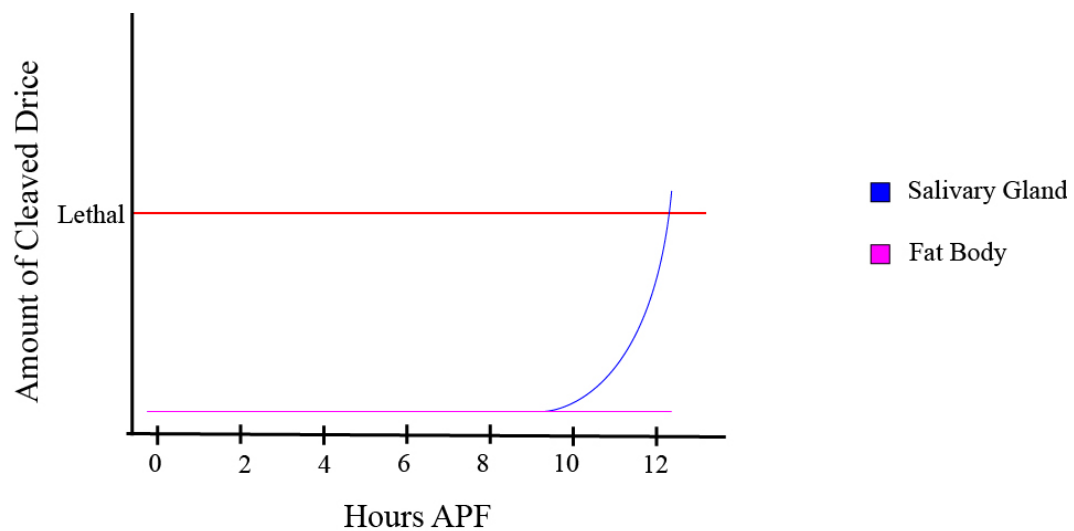


**Figure 8. Scenario 1.** Levels of cleaved Drice in the fat body do not change during metamorphosis.

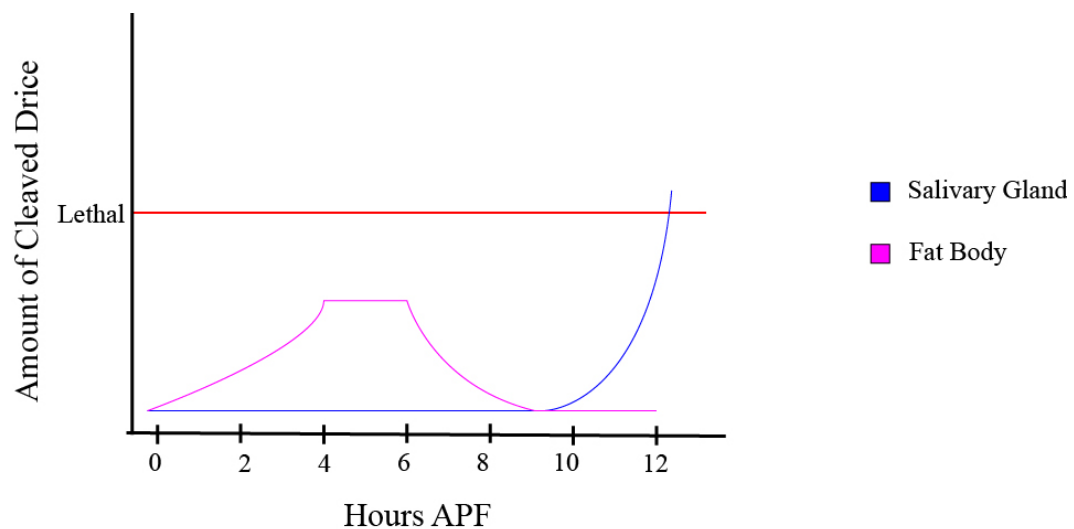


**Figure 9. Scenario 2a.** Levels of cleaved Drice in the fat body are at their highest between 4-6 APF.

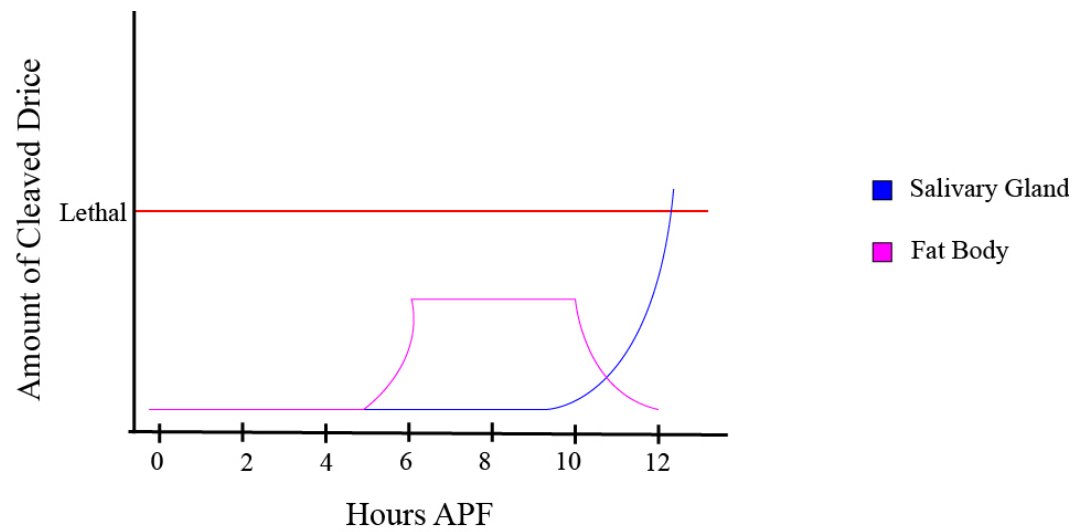


**Figure 10. Scenario 2b.** Levels of cleaved Drice in the fat body are at their highest between 6-10 APF.

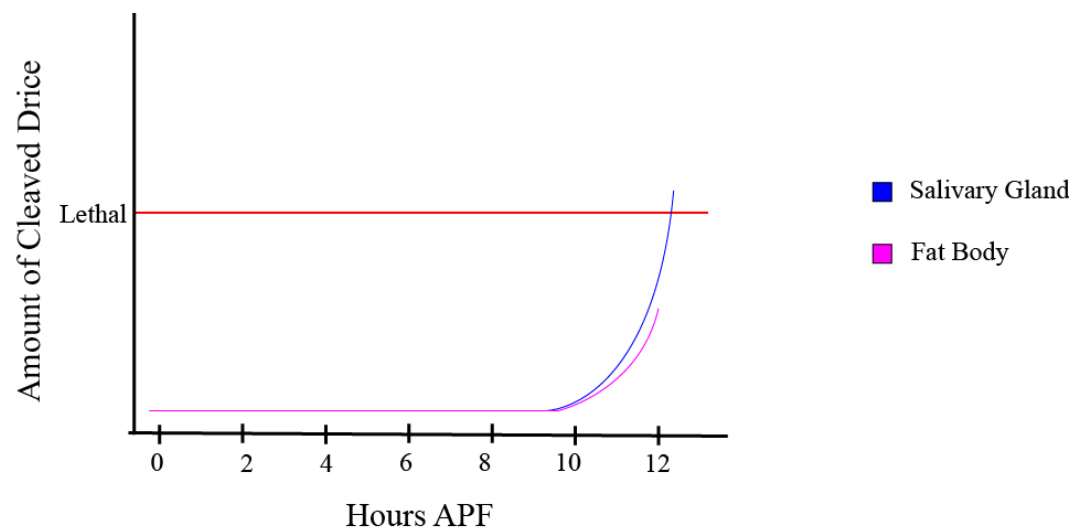


**Figure 11. Scenario 3.** Levels of cleaved Drice in the fat body are at their highest at 12 APF.

## LITERATURE CITED

Aguila, J. R., Suszko, J., Gibbs, A. G., & Hoshizaki, D. K. (2007). The role of larval fat cells in adult *drosophila melanogaster*. *Journal of Experimental Biology*, *210*(6), 956–963. <https://doi.org/10.1242/jeb.001586>

Alexander, G. (2021). Genetic Analysis of Programmed Cell Death. Mount Holyoke College.

Berry, D. L., & Baehrecke, E. H. (2007). Growth arrest and autophagy are required for salivary gland cell degradation in *drosophila*. *Cell*, *131*(6), 1137–1148. <https://doi.org/10.1016/j.cell.2007.10.048>

Bond, N. D., Nelliott, A., Bernardo, M. K., Ayerh, M. A., Gorski, K. A., Hoshizaki, D. K., & Woodard, C. T. (2011).  $\beta$ FTZ-F1 and matrix metalloproteinase 2 are required for fat-body remodeling in *drosophila*. *Developmental Biology*, *360*(2), 286–296. <https://doi.org/10.1016/j.ydbio.2011.09.015>

Cashio, P., Lee, T. V., & Bergmann, A. (2005). Genetic control of programmed cell death in *Drosophila melanogaster*. *Seminars in Cell & Developmental Biology*, *16*(2), 225–235. <https://doi.org/10.1016/j.semcdb.2005.01.002>

Chen, M., Rong, R., & Xia, X. (2022). Spotlight on pyroptosis: Role in pathogenesis and therapeutic potential of ocular diseases. *Journal of Neuroinflammation*, *19*(1). <https://doi.org/10.1186/s12974-022-02547-2>

Eskandari, E., & Eaves, C. J. (2022). Paradoxical roles of caspase-3 in regulating cell survival, proliferation, and tumorigenesis. *The Journal of Cell Biology*, *221*(6), e202201159. <https://doi.org/10.1083/jcb.202201159>

Han, A. (2019). The Role of the Caspase Dronc and Inhibitor of Apoptosis (Diap1) in Programmed Cell Death (PCD) of *Drosophila melanogaster*. Mount Holyoke College.

Hengartner, M. O. (2000). The biochemistry of apoptosis. *Nature*, *407*(6805), 770–776. <https://doi.org/10.1038/35037710>

Hirata, Y., Cai, R., Volchuk, A., Steinberg, B. E., Saito, Y., Matsuzawa, A., Grinstein, S., & Freeman, S. A. (2023). Lipid peroxidation increases

membrane tension, piezo1 gating, and cation permeability to execute ferroptosis. *Current Biology*, 33(7), 1282–1294.

<https://doi.org/10.1016/j.cub.2023.02.060>

Jennings, B. H. (2011). *Drosophila* – a versatile model in Biology & Medicine. *Materials Today*, 14(5), 190–195. [https://doi.org/10.1016/s1369-7021\(11\)70113-4](https://doi.org/10.1016/s1369-7021(11)70113-4)

Khalid N & Azimpouran M. (2023) Necrosis. *StatPearls [Internet]*.

StatPearls Publishing; 2023 Jan-.

<https://www.ncbi.nlm.nih.gov/books/NBK557627/>

Kiran Cavale, S. (2022). Independent Study Paper. Mount Holyoke College.

Nelliot, A., Bond, N., & Hoshizaki, D. K. (2006). Fat-body remodeling in *drosophila melanogaster*. *Genesis*, 44(8), 396–400.

<https://doi.org/10.1002/dvg.20229>

NHGRI. (2023, April 18). *Apoptosis*. Genome.gov. Retrieved April 21, 2023, from <https://www.genome.gov/genetics-glossary/apoptosis>

Ojha, S., & Tapadia, M. G. (2021). Nonapoptotic role of caspase-3 in regulating rho1gtpase-mediated morphogenesis of epithelial tubes of *Drosophila* renal system. *Developmental Dynamics*, 251(5), 777–794.

<https://doi.org/10.1002/dvdy.437>

Salvesen, G. S., & Abrams, J. M. (2004). Caspase activation – stepping on the gas or releasing the brakes? lessons from humans and flies. *Oncogene*, 23(16), 2774–2784.

<https://doi.org/10.1038/sj.onc.1207522>

Yalonetskaya, A., Mondragon, A. A., Elguero, J., & McCall, K. (2018). I Spy in the Developing Fly a Multitude of Ways to Die. *Journal of Developmental Biology*, 6(4), 26. <https://doi.org/10.3390/jdb6040026>

Zachariou, A., Tenev, T., Goyal, L., Agapite, J., Steller, H., & Meier, P. (2003). IAP-antagonists exhibit non-redundant modes of action through differential diap1 binding. *The EMBO Journal*, 22(24), 6642–6652.

<https://doi.org/10.1093/emboj/cdg617>